Computation of the Sommerfeld Integral Tails Using the Matrix Pencil Method

Mengtao Yuan and Tapan K. Sarkar

***Abstract*—The oscillating infinite domain Sommerfeld integrals (SI) are difficult to integrate using a numerical procedure when dealing with structures in a layered media, even though several researchers have attempted to do that. Generally, integration along the real axis is used to compute the SI. However, significant computational effort is required to integrate the oscillating and slowly decaying function along the tail. Extrapolation methods are generally applied to accelerate the rate of convergence of these integrals. However, there are difficulties with the extrapolation methods, such as locations for the breakpoints. In this paper, we illustrate a simplified approach for accurate and efficient calculation of the integrals dealing with the tails of the SI. In this paper, we fit the tail by a sum of finite (usually 10 to 20) complex exponentials using the matrix pencil method (MPM). The integral of the tail of the SI is then simply calculated by summing some complex numbers. No numerical integration is needed in this process, as the integrals can be done analytically. Good accuracy is achieved with a small number of evaluations for the integral kernel (60 points for the MPM as compared with hundreds or thousands of functional evaluations using the traditional extrapolation methods) along the tails of the SI. Simulation results show that to obtain the similar accuracy in the evaluation of the SI, the MPM is approximately 10 times faster than the traditional extrapolation methods. Moreover, since the MPM is robust to the effects of noise, this method is more stable, especially for large values of the horizontal distances. The method proposed in this paper is thus a new and better technique to obtain accurate results for the computation of the Green's function for a layered media in the spatial domain.**

***Index Terms*—Extrapolation methods, matrix pencil method (MPM), method of moments (MoM), Sommerfeld integration (SI).**

I. Introduction

Among the different numerical tools used in computational electromagnetics for handling layered dielectric regions, the method of moments (MoM) is one of the most efficient. It provides stable and accurate results while using less number of unknowns (for example, in [1]–[3]). Basically two main steps are involved in MoM, one is to fill up the dense matrix and the other is to solve it. The second step usually takes the dominant computational load for dealing with objects in an inhomogeneous media. However, for objects placed in a multilayered media or microstrip structures, the spatial-domain Green's function required in matrix filling is complicated by the stratified structures. The SI is then introduced to calculate each element of the Dyadic Green's functions [4]–[7]. The SI is semi-infinite integral involving Bessel functions of the first kind (or infinite integral for Hankel functions). Due to the oscillating and slowly decaying property of the integrands, the computation of the SI is very time consuming. In some multilayered MoM calculations, the CPU time for matrix filling is larger than the time for solving the matrix.

Much effort has been focused on the simplification of the SI. One of these ideas is to avoid the numerical integrations by approximating the integrands or a part of the integrand with some simple functions. Then these approximations of the SI can be integrated analytically [8]–[13]. Bessel and Hankel functions have asymptotic sinusoidal forms for large arguments, which can be used to obtain closed-form Green's functions [8]. These asymptotic methods have the disadvantage of less accuracy, especially for small distances between the source and the field points. Plane wave expansion method was introduced in [9], but it is valid only for distances less than 1.5 λ. The discrete complex image method (DCIM) was developed to avoid the numerical computation of the SI [10]. The quasistatic and surface-wave terms are extracted first. Instead of approximating the whole integrand, DCIM expands the spectral domain Green's function by a sum of complex exponentials. The closed-form of the Green's function in spatial domain is then obtained analytically by the use of the Sommerfeld identity. However, in DCIM, the approximation of the spectral kernel is implemented through a concaved finite contour instead of using a contour to infinity. The accuracy is sensitive to parameters such as, the slope of the contour [11]. There are difficulties in the extraction of surface-wave components and there are errors in the near-field region due to the singularity of the Hankel functions [12]. Moreover, without the extraction of the surface-wave terms, DCIM cannot express the Green's function (GF) in the far field region. The study of DCIM also requires rigorous results from other methods as a verification of the performance. Another DCIM applied directly in k_ρ domain was proposed in [13]. It has the same disadvantage as the original DCIM of accuracy in the far-field region.

Attention is directed back to the classical numerical methods for the computation of the SI using some of the other methods, which is time consuming but provides the most accurate result. Since the integrands in the SI are defined in the complex domain, various paths of integration can be employed (for example, in [14]), but the real-axis path, indented into the first quadrant to avoid the branch-point and pole singularities, has proven to be the most convenient for multilayered media [7]. A significant part of the computation involves the integration of the tail, because it is oscillating and slowly decaying to infinity. A solution for this difficulty is to integrate finite segments of it and get a series. Then use an extrapolation method to accelerate the convergence of the series. Methods of extrapolation for the tails of the SI have been exclusively analyzed and the results summarized in [15]. Although the acceleration by extrapolation works well in most cases, it suffers from the computational load of numerical integration. Moreover, the accuracy of the extrapolation is sensitive to the choice of the break points in the path of integration and the value of the horizontal distances from the source point.

The goal of this paper is to provide an accurate and efficient method to integrate the SI at least as rigorously as the extrapolation method, but in a much faster but robust fashion. We observe that the oscillating and slowly decaying tails of the SI behave similar to a complex exponential function with the exponent having a negative real part. Since the integrals of the exponential functions can be easily calculated and the values of these exponentials are zeros at infinity, we can first approximate the integrands by a sum of complex exponentials. It is different from the approximations used in DCIM. The approximation for this method is done directly to the whole integrand. Hence it is a more straightforward method. Among the many methods of approximating a function by a sum of complex exponentials, we choose the matrix pencil method (MPM) since it is robust to noise and computationally efficient [13]. Numerical results show that only 60 samples (or functional evaluations) and 10 to 20 exponential functions are enough to obtain an accuracy comparable to the traditional extrapolation methods. The CPU time for the MPM with this small number of samples and exponents is very small. Moreover, MPM is more robust to the variation in the value of the horizontal distance ρ. Satisfactory results have been obtained for electrically large objects in inhomogeneous media by MoM [2], [3], but analysis of large objects in multilayered media is impeded by the excessive computational effort and the accuracy for large ρ. It is shown in this paper that MPM is robust for ρ from 10^{-4} wavelengths to more than 160 wavelengths, which is suitable for analysis for large structures in MoM.

Manuscript received September 29, 2005; revised December 1, 2005.

The authors are with the EECS Department, Syracuse University, Syracuse, NY 13244 USA (e-mail: myuan@syr.edu; tksarkar@syr.edu).

Digital Object Identifier 10.1109/TAP.2006.872656

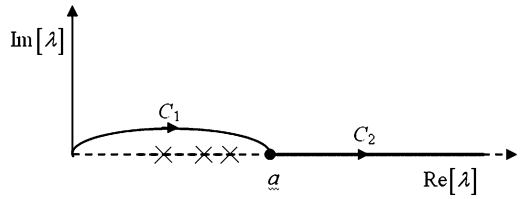

Fig. 1. Path for typical Sommerfeld integration.

We organize this paper as follows. The nature of the SI and the extrapolation methods are briefly discussed in Section II. The MPM and its application to the evaluation of the SI is explained in Section III. Using numerical results we show the performance of the MPM and compare it to the traditional extrapolation methods and DCIM in Section IV. Finally some conclusions are drawn in Section V.

II. Sommerfeld Integrals and the Extrapolation Methods

In the mixed potential integral equations (MPIE) used in MoM [7], the spatial domain dyadic Green's functions (DGF) associated with the vector or the scalar potentials at a field point $\mathbf{r}$ due to an arbitrary oriented source at $\mathbf{r}'$ in a layer of stratified media can be expressed by a Sommerfeld-type integral [15]

$$I = \int_0^\infty \tilde{G}(z, z'; \lambda) J_n(\lambda\rho)\lambda d\lambda, \quad n = 0, 1, 2 \tag{1}$$

where $\tilde{G}$ is the spectral domain Green's function. J_n is the nth order Bessel functions of the first kind. λ is the radial wave number and ρ is the horizontal distance between the field and source points in the xOy plane. z and z' are the vertical components for $\mathbf{r}$ and $\mathbf{r}'$ respectively.

The most convenient path to compute the integral in (1) is along the indented path in the first quadrant to avoid singularities from 0 to a, and then from a to ∞ along the real axis, assuming that there are no singularities on $[a, \infty)$. Choice of the path along $[0, a]$ is not critical [17], as long as the singularities are circled around and the imaginary part of λ on the path is positive and not too large to handle large values of J_n. We choose an elliptical path C_1 for integration as shown in Fig. 1. According to the residue theorem for complex functions, the singularities of the spectral domain GF are accurately included in the result of the integration. This feature differs from the DCIM method. In the DCIM method, the complex images are approximately obtained by a set of samples of the spectral GF. This kind of approximation is not accurate enough to include the information of the singularities [10]–[13], especially in the far field region. This point is also illustrated by numerical examples in Section IV. Moreover, the direct numerical integration of the SI is still the best choice to obtain the most rigorous results.

Since we can do the finite numerical integration on $[0, a]$ quite easily and accurately, we focus on the more difficult integration on the path $[a, \infty)$. The integrand in (1) is given by

$$f(\lambda) = \tilde{G}(z, z'; \lambda) J_n(\lambda\rho)\lambda. \tag{2}$$

In some situations $f(\lambda)$ is not convergent, i.e., $\lim_{\lambda\to\infty} |f(\lambda)| = \infty$, but we can extract the divergent term easily (for example, the static term in [10] or [18]). In this paper, we assume $f(\lambda)$ is convergent, such that $\lim_{\lambda\to\infty} |f(\lambda)| = 0$.

Bessel functions have the following asymptotic forms for large arguments:

$$J_n(\lambda\rho) \approx \sqrt{2/(\pi\lambda\rho)}\cos(\lambda\rho - n\pi/2 - \pi/4), \quad \text{for } \lambda\rho \gg 1 \frac{n!}{r!(n-r)!}. \tag{3}$$

They decay at the rate $\sqrt{2/(\pi\lambda\rho)}$ and have the asymptotic half period $q = \pi/\rho$. The proven and most popular method to integrate $f(\lambda)$ on $[a, \infty)$ is the traditional "extrapolation method." This is based on integrating $f(\lambda)$ during the first several half periods, accumulating them to obtain a series whose sum is evaluated using some transforms to accelerate the convergence of the series [15]. Note that the numerical integration is performed only on $[a, b]$ where $b = a + Kq$ and K is a finite integer. The extrapolation transforms the integration result on $[a, b]$ to the final result on $[a, \infty)$. Problems arise on how to define the location of the "break points" on the path and how to define each half period. For different kinds of break points, (for example, the extremes or zeros of J_n), the traditional extrapolation method is likely to have different computational errors.

III. Use of the Matrix Pencil Method to Compute the Sommerfeld Integrals

The MPM [16] can be viewed as a new extrapolation method to compute the tails of the SI, since the evaluations of $f(\lambda)$ on $[a, b]$ are also used to perform the integration along $[a, \infty)$.

Suppose we have m samples of $f(\lambda)$ per half period. We have a total of $N = mK$ samples, and $t = \lambda - a$. We can approximate $f(t)$ on $[0, \infty)$ by a sum of M exponentials as

$$f(t) \approx \sum_{i=1}^{M} R_i e^{s_i t}; \quad 0 \le t < \infty \tag{4}$$

where R_i is called the residue or the complex amplitude, and s_i is the exponent. For the assumption in Section II, $\lim_{t\to\infty} |f(t)| = 0$, so $Re[s_i] < 0$. If we sample (4) with a sampling step $\Delta T = q/m$, then (4) becomes

$$f_p = f(p\Delta T) = \sum_{i=1}^{M} R_i \gamma_i^p, \text{for } p = 0, 1, \ldots, N-1 \tag{5}$$

where the poles are $\gamma_i = e^{s_i \Delta T}$ for $\mathrm{i} = 1, 2, \ldots, \mathrm{M}$.

To solve for the R_i and s_i using $\{f_p\}$, we first construct the Hankel matrix as

$$\mathbf{Y} = \begin{bmatrix} f_0 & f_1 & \cdots & f_L \\ f_1 & f_2 & \cdots & f_{L+1} \\ \vdots & \vdots & & \vdots \\ f_{N-L-1} & f_{N-L} & \cdots & f_{N-1} \end{bmatrix} \tag{6}$$

and perform a singular value decomposition (SVD) of $\mathbf{Y}$,

$$\mathbf{Y} = \mathbf{U}\mathbf{\Sigma}\mathbf{V}^H \tag{7}$$

where the superscript H defines the conjugate transpose of a matrix and $\mathbf{\Sigma}$ is a diagonal matrix with singular values σ_i of $\mathbf{Y}$. L is the pencil parameter and we choose $L = N/2$ in this paper. How to choose this parameter has been discussed in [20]. The number of exponentials M can be chosen by analyzing the values of σ_i. We can set a tolerance tol, and discard the small σ_i, which are $\sigma_i/\sigma_{\max} < \mathrm{tol}$, where $\sigma_{\max}$ is the largest singular value. tol can be used to adaptively control the accuracy of the SI. Smaller tol means larger number of exponentials is used to approximate $f(t)$ and yield more accurate results for the SI, but requires longer computational time. Once M is decided, the first M columns of U are used to build a new $M \times M$ matrix using a least squares method, and the eigenvalues of this matrix are the poles γ_i. R_i are solved from the least squares problem

$$\begin{bmatrix} 1 & 1 & \cdots & 1_L \\ \gamma_1 & \gamma_2 & \cdots & \gamma_M \\ \vdots & \vdots & & \vdots \\ \gamma_1^{N-1} & \gamma_2^{N-1} & \cdots & \gamma_M^{N-1} \end{bmatrix} \begin{bmatrix} R_1 \\ R_2 \\ \vdots \\ R_M \end{bmatrix} = \begin{bmatrix} f_1 \\ f_2 \\ \vdots \\ f_{N-1} \end{bmatrix}. \tag{8}$$

The s_i can be obtained from

$$s_i = \log(\gamma_i)/\Delta T. \tag{9}$$

Once R_i and s_i are solved for, the integration of $f(\lambda)$ on $[a,\infty)$ can be simply calculated analytically through

$$\int_a^\infty f(\lambda)d\lambda = \int_0^\infty f(t)dt \approx \sum_{i=1}^{M}\int_0^\infty R_i e^{s_i t}dt = -\sum_{i=1}^{M}\frac{R_i}{s_i} \tag{10}$$

with the assumption $Re[s_i] < 0$. There are three dominant computational loads: first in the computation of the SVD in (6), second in the eigenvalue solver for γ_i and the third in the least squares solver for R_i in (8). For large L and M, the computational effort for these three steps is the most time consuming. Fortunately, the tails of the SI have shapes which are suitable for MPM. Simulation results in the next section show that $N = 60(L = 31)$ and $M \approx 20$ are enough to obtain satisfactory accuracy for this integration. With this method, eigenvalue and least squares solvers for a 20×20 matrix can be performed with trivial computational effort.

The fundamental differences between MPM and the traditional extrapolation methods in [15] are as follows.

A) No splits of half periods are necessary. There is no need to find the optimal locations for the break points.

B) The whole set of samples on $[a,b]$ are used at one time to solve the parameters of the exponentials.

C) The exponentials obtained are used to fit $f(\lambda)$ on the entire domain of $[a,\infty)$.

D) There is no numerical integration of the tails of the SI with the MPM method and the matrix computations become trivial.

Because of these features, one would expect that MPM is more robust and efficient than traditional extrapolation methods. This expectation is validated by numerical results in the next section.

IV. Numerical Results

In this section, we show the accuracy and CPU times used for MPM for integration of the tails of the SI, and we compare these two performance parameters to results obtained by one of the most efficient traditional extrapolation methods.

We use the same examples as in [15]. The simplest of the SI is the Sommerfeld identity [4]. Suppose we have the following SI

$$\int_a^\infty \frac{e^{-jk_z|z|}}{jk_z}J_0(\lambda\rho)\lambda d\lambda = \frac{e^{-jkr}}{r} - \int_0^a \frac{e^{-jk_z|z|}}{jk_z}J_0(\lambda\rho)\lambda d\lambda \tag{11}$$

where $r = \sqrt{\rho^2+z^2}$ and $k_z = \sqrt{k^2-\lambda^2}$. $k = k_0\sqrt{\varepsilon}$ is the wave number in the media with dielectric constant ε, where k_0 is the wave number in free space. We choose $\varepsilon = 16 - j0.1$. There is a singularity at $\lambda = k_0\sqrt{\varepsilon}$. To avoid this singularity, the integration of the right hand side of (11) is computed along the path from 0 to a shown in Fig. 1. It is integrated to machine accuracy by using the adaptive Lobbatto quadrature [21]. The integration for the tail starts at a.

We choose the most critical case as $z = 0$, in which case the tail is oscillating and slowly decaying to 0 as $\lambda \to \infty$. The remaining parameters to be decided are the samples $\{f_p\}$ used as inputs for MPM. Simulation shows that stable and accurate results can be obtained by equally sampling $f(\lambda)$ with $m = 6$ points per half period, and $K = 10$ half periods are good enough for the extrapolation from b to ∞. Hence the total number of evaluations of the integrand is $N = 60$. Fig. 2 shows the real part of the 60 samples of the tails used in MPM for $k_0\rho = 0.01$ and $k_0\rho = 100$. The two series of samples show the similar oscillating and slow decaying shape. For larger $k_0\rho$, the rate of decay is smaller.

Note that the plots shown in Fig. 2 are typical tails of the SI. Additional real forms of the SI for a stratified media due to horizontal or vertical sources have also been computed by using the MPM but not shown in this paper. The inputs to the MPM for these other examples look similar to Fig. 2 and the integration results are stable and accurate.

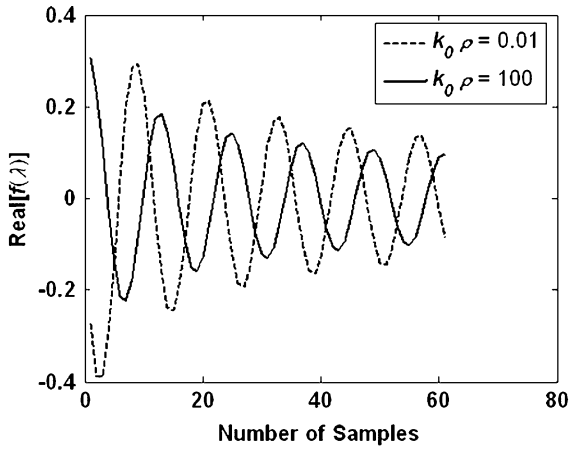

Fig. 2. Samples of the tails of the Sommerfeld integral used in MPM.

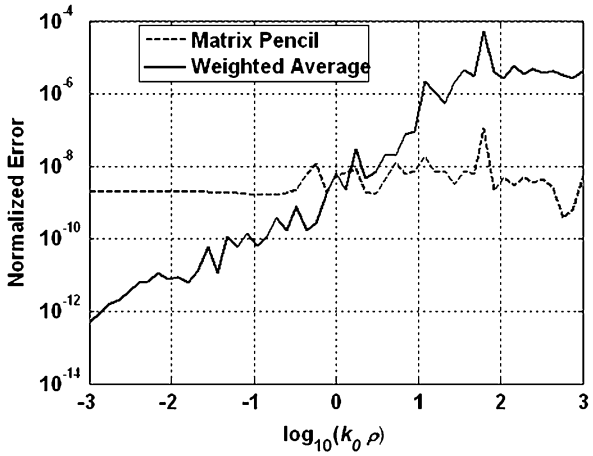

Fig. 3. Normalized errors for the tail integration, $\mathrm{tol} = 10^{-14}$.

Simulation results are shown Figs. 3 through 7 for different values of tol along $k_0\rho$ from 10^{-3} to 10^3. Note that $k_0 = 2\pi/\lambda_0$ where λ_0 is the wavelength in free space. Hence ρ varies from around $1.6 \times 10^{-4}\ \lambda_0$ to 160 λ_0. The integration results on the left hand side of (11) are compared with the results obtained from the right hand side, and the normalized errors are plotted. Among the various traditional extrapolation methods listed in [15], the weighted-average method (WAM) is one of *the most versatile and efficient convergence accelerators for evaluation of the tails of the Sommerfeld integrals*. For this reason, we chose to compare the performance of the asymptotic WAM to the proposed MPM method. Recall that the parameter tol is the tolerance, related to the ratio of the singular values in MPM. This parameter is also applied as a measure of relative error for adaptive Lobbatto quadrature used for integration in each half period in WAM. As in [15], the number of half periods is set to 10 for both methods.

Fig. 3 shows the normalized errors for MPM and WAM when $\mathrm{tol} = 10^{-14}$. The performance of WAM is better when $k_0\rho$ is small. However, when $k_0\rho$ is larger than 1 ($\rho > 0.16\lambda_0$), MPM has better accuracy than WAM. Moreover, MPM is more stable than WAM when $k_0\rho$ increases. The normalized error of MPM remains below 10^{-7} for all $k_0\rho$.

The CPU-times of both methods are shown in Fig. 4. To calculate the integrals to $\mathrm{tol} = 10^{-14}$, MPM is generally 19 times faster than WAM. An average of 17 exponentials are required to approximate $f(\lambda)$. The dominant computational time of WAM is spent on the evaluation of

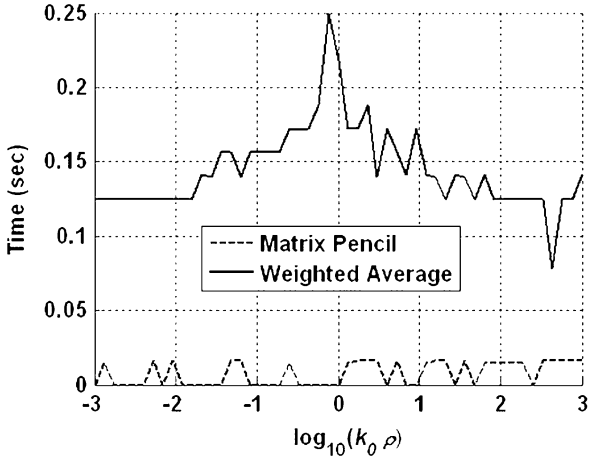

Fig. 4. Comparison of CPU times for the two methods, $\mathrm{tol} = 10^{-14}$.

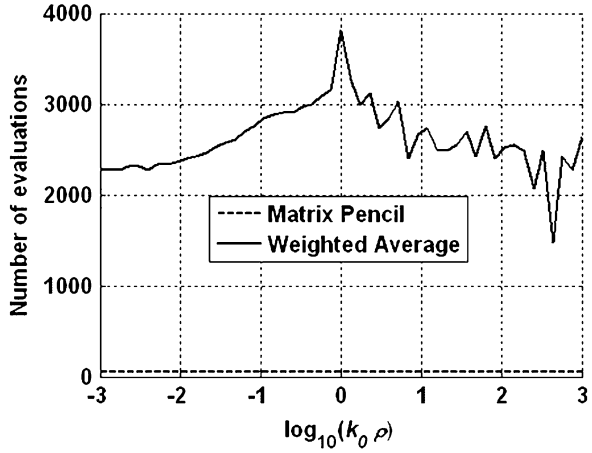

Fig. 5. Number of functional evaluations for the two methods, $\mathrm{tol} = 10^{-14}$.

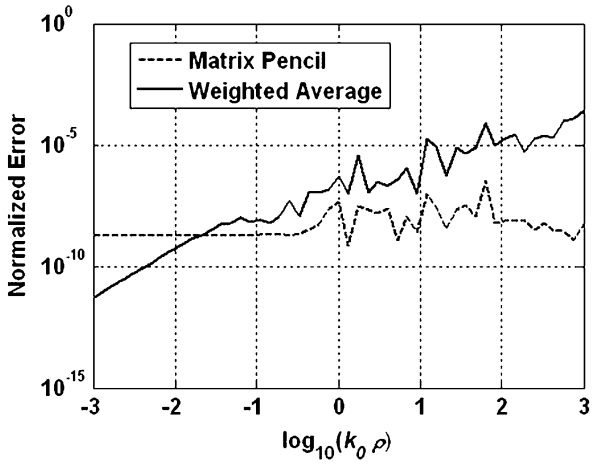

Fig. 6. Normalized errors for the tail integrations, $\mathrm{tol} = 10^{-12}$.

the integrand. Fig. 5 shows that thousands of integrand evaluations are required for WAM compared to a constant 60 evaluations for MPM.

When tol becomes higher from 10^{-14} to 10^{-10}, the performance of MPM remains consistent, as shown in Figs. 6 and 7. However, the performance of WAM deteriorates. For $\mathrm{tol} = 10^{-12}$ as in Fig. 6, the accuracy of MPM is better than WAM for most $k_0\rho$, and the CPU-time for WAM averages 8 times longer than MPM. An average of 14.5 exponential functions are required to approximate $f(\lambda)$. For $\mathrm{tol} = 10^{-10}$, the CPU-time used for WAM is 2 times longer than MPM since less evaluations of the integrand is necessary, but the performance of WAM

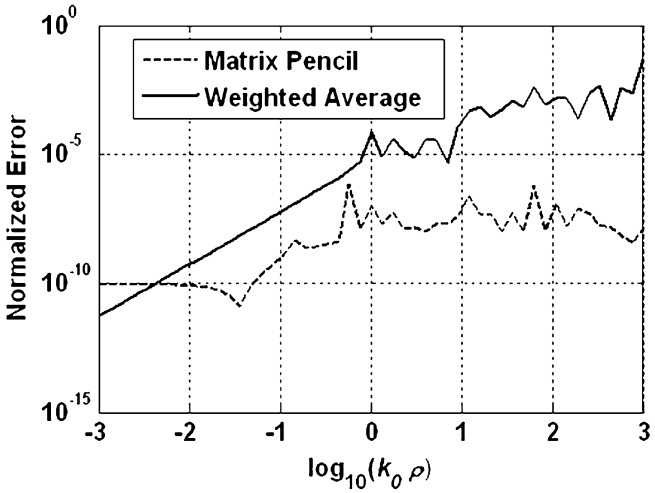

Fig. 7. Normalized errors for the tail integrations, $\mathrm{tol} = 10^{-10}$.

Layer	ε_r	h
7	1	∞
6	2.2	0.7 mm
5	10	0.2 mm
4	7	0.3 mm
3	12.5	0.3 mm
2	10	0.5 mm
1	8.6	0.4 mm
PEC		

Fig. 8. Stratified structure of the 7-layer media.

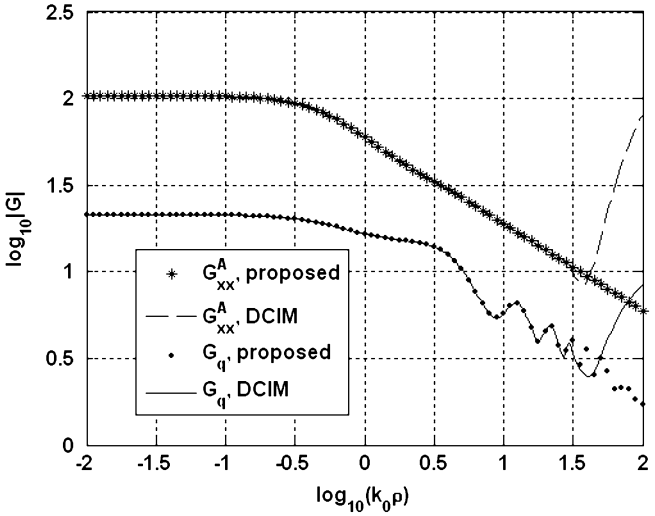

Fig. 9. Performance comparison between the proposed method and the DCIM method.

is even worse. An average of 13 exponentials are required to approximate $f(\lambda)$ when $\mathrm{tol} = 10^{-10}$. Based on the numerical results shown in Figs. 3–7, we can observe that MPM is generally more accurate than WAM. MPM has two additional advantages: greater robustness and faster computational time.

As another example, we use a complex problem and compare the results of the proposed method to the DCIM. We analyze the spatial domain GF for a 7-layer media. The stratified media is described in Fig. 8. The source is located at $z' = 1$ mm (in the second layer) and the field point is located at $z = 2$ mm (in the sixth layer). The x component of the vector potential GF (G^A_{xx}) due to a horizontal source and the scalar potential GF (G_q) are shown in Fig. 9. The results of the DCIM method is not correct for larger values of ρ. The reason for this

is explained in Section II. The results obtained by WAM are slightly different from those obtained by the proposed method. The WAM results are not shown in Fig. 9 because they essentially overlay with that of the proposed method. However, the CPU time used in WAM is 10–15 times faster than MPM. Also, from Figs. 3 through 7 we see that use of MPM in the computation of the SI provides more accurate results.

V. Conclusion

An adaptive, efficient and robust method is introduced to compute the tails of the SI. It uses the MPM to extrapolate the tail using a few known samples, and the integration on $[a, \infty)$ is analytically computed from the sum of complex exponentials. Compared with the traditional extrapolation methods, MPM does not require the difficult task of locating the optimal break points. Moreover, MPM uses the whole data, and the poles and residues are computed using a least squares method. Hence, MPM is more robust and efficient than any of the other extrapolation methods available in current publications. The integration of the tails remains accurate for horizontal distances greater than 160 wavelengths, an achievement which no other method can claim; hence it is capable of providing rigorous results for MoM applied to large structures in a multilayered media.

Acknowledgment

The authors thank Ms. M. C. Taylor for her careful proofreading of this paper.

References

[1] B. M. Kolundzija and A. R. Djordjevic, *Electromagnetic Modeling of Composite Metallic and Dielectric Structures*. Boston, MA: Artech House, 2002.

[2] M. Yuan, T. K. Sarkar, and B. M. Kolundzija, "Modeling large and complex structures in computational electromagnetics," IEEE Antennas Propagat Mag, submitted for publication.

[3] WIPL-D Ltd., *WIPL-D Pro User's Manual*, 2004.

[4] A. Sommerfeld, *Partial Differential Equations in Physics*. New York: Academic Press, 1969.

[5] T. K. Sarkar, "Analysis of arbitrarily oriented thin wire antenna arrays over imperfect ground planes," Ph.D. dissertation, Syracuse Univ., 1975.

[6] W. C. Chow, *Waves and Fields in Inhomogeneous Media*. New York: Van Nostrand, 1990.

[7] K. A. Michalski and J. R. Mosig, "Multilayered media Green's functions in integral equation formulations," *IEEE Trans. Antennas Propag.*, vol. 45, no. 3, pp. 508–519, Mar. 1997.

[8] S. Barkeshli, P. H. Pathak, and M. Marin, "An asymptotic closed-form microstrip surface Green's function for the efficient moment method analysis of mutual coupling in microstrip antenna," *IEEE Trans. Antennas Propag.*, vol. 38, no. 9, pp. 1374–1383, Sep. 1990.

[9] M. Ayatollahi and S. Safavi-Naeini, "A new representation for the Green's function of multilayer media based on plane wave expansion," *IEEE Trans. Antennas Propag.*, vol. 52, no. 6, pp. 1548–1557, Jun. 2004.

[10] Y. L. Chow, J. J. Yang, D. G. Fang, and G. E. Howard, "A closed-form spatial Green's function for the thick microstrip substrate," *IEEE Trans. Microw. Theory Tech.*, vol. 39, no. 3, pp. 588–592, Mar. 1991.

[11] M. I. Aksun, "A robust approach for the derivation of closed-form Green's functions," *IEEE Trans. Microwave Theory Tech.*, vol. 44, no. 5, pp. 651–658, May 1996.

[12] F. Ling and J.-M. Jin, "Discrete complex image method for Green's functions of general multilayer media," *IEEE Microw. Guided Wave Lett.*, vol. 10, pp. 400–402, Oct. 2000.

[13] Y. Ge and K. P. Esselle, "New closed-form Green's functions for microstrip structures—Theory and results," *IEEE Trans. Microw. Theory Tech.*, vol. 50, pp. 1556–1560, Jun. 2002.

[14] T. J. Cui and W. C. Chew, "Fast evaluation of sommerfeld integrals for EM scattering and radiation by three-dimensional buried objects," *IEEE Trans. Geosci. Remote Sensing*, vol. 37, pp. 887–900, Mar. 1999.

[15] K. A. Michalski, "Extrapolation methods for Sommerfeld integral tails," *IEEE Trans. Antennas Propag.*, vol. 46, no. 10, pp. 1405–1418, Oct. 1998.

[16] T. K. Sarkar and O. Pereira, "Using the matrix pencil method to estimate the parameters of a sum of complex exponentials," *IEEE Antennas Propag. Mag.*, vol. 37, no. 2, pp. 48–55, Feb. 1995.

[17] P. Gay-Balmaz and J. R. Mosig, "3-D planar radiating structures in stratified media," *Int. J. Microw. Millimeter-Wave Comput.-Aided Eng.*, vol. 7, pp. 330–343, Sep. 1997.

[18] J. R. Mosig and T. K. Sarkar, "Comparison of quasistatic and exact electromagnetic fields from a horizontal electric dipole above a lossy dielectric backed by an imperfect ground plane," *IEEE Trans. Microw. Theory Tech.*, vol. 34, pp. 379–387, Apr. 1986.

[19] G. H. Golub and C. F. Van Loan, *Matrix Computations*. Baltimore, MD: John Hopkins Univ. Press, 1983.

[20] Y. Hua and T. K. Sarkar, "Matrix pencil method for estimating parameters of exponentially damped/undapmed sinusoids in noise," *IEEE Trans. Acoust., Speech and Signal Processing*, vol. 38, pp. 814–824, May 1991.

[21] W. Gander and W. Gautschi, "Adaptive Quadrature - Revisited," *BIT*, vol. 40, no. 1, pp. 84–101, Mar. 2000.